Electronic Supplementary Material (ESI) for Journal of Materials Chemistry A.

Supporting Information

Two different mechanisms of $CH_3NH_3PbI_3$ film formation in one-step deposition and its effect on photovoltaic properties of OPV-type perovskite solar cells

Seunghwan Bae,[a] Seung Jin Han,[a] Tae Joo Shin,[b] and Won Ho Jo*[a]

[a]*Department of Materials Science and Engineering, Seoul National University, 1 Gwanak-ro, Gwanak-gu, Seoul 151-744, Korea*

[b]*Pohang Accelerator Laboratory, Pohang, Kyungbuk 790-784, Korea*

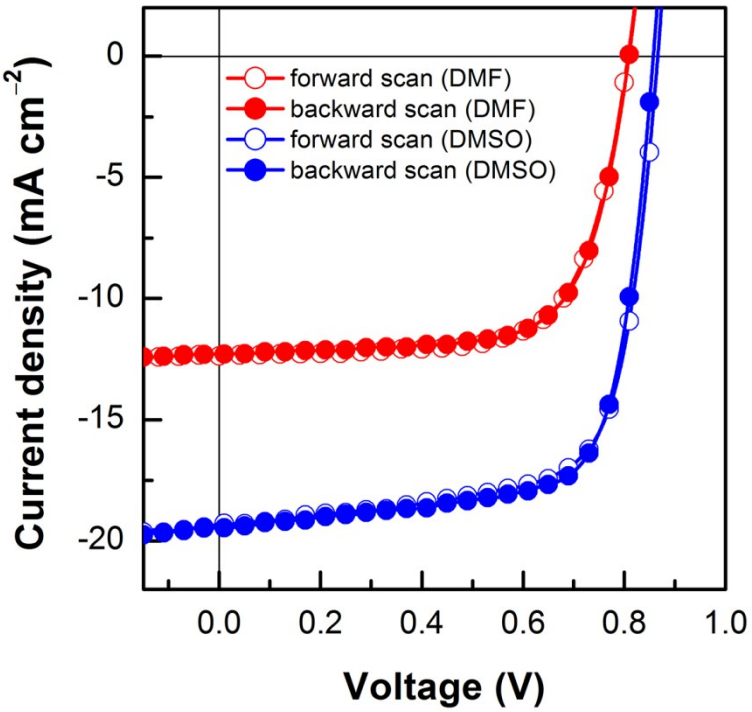

Fig. S1. *J–V* hysteresis of perovskite solar cells fabricated from DMF and DMSO solution. The $CH_3NH_3PbI_3$ films are prepared by spin-coating at 3000 rpm for 3 s (DMF) and 15 s (DMSO), respectively and are thermally treated at 110 °C for 30 s.

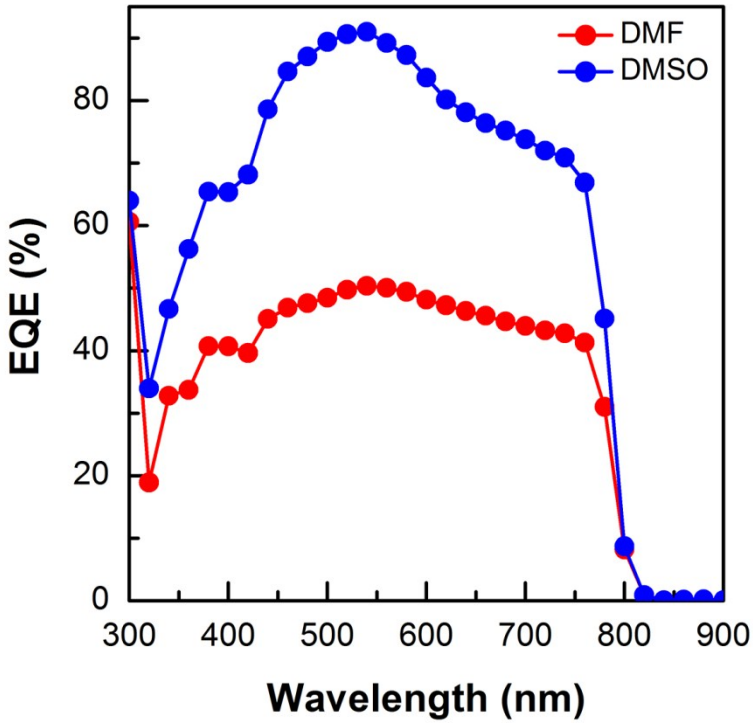

Fig. S2. External quantum efficiency spectra of the best cells fabricated from DMF and DMSO solution. The $CH_3NH_3PbI_3$ films are prepared by spin-coating at 3000 rpm for 3 s (DMF) and 15 s (DMSO), respectively and are thermally treated at 110 °C for 30 s.

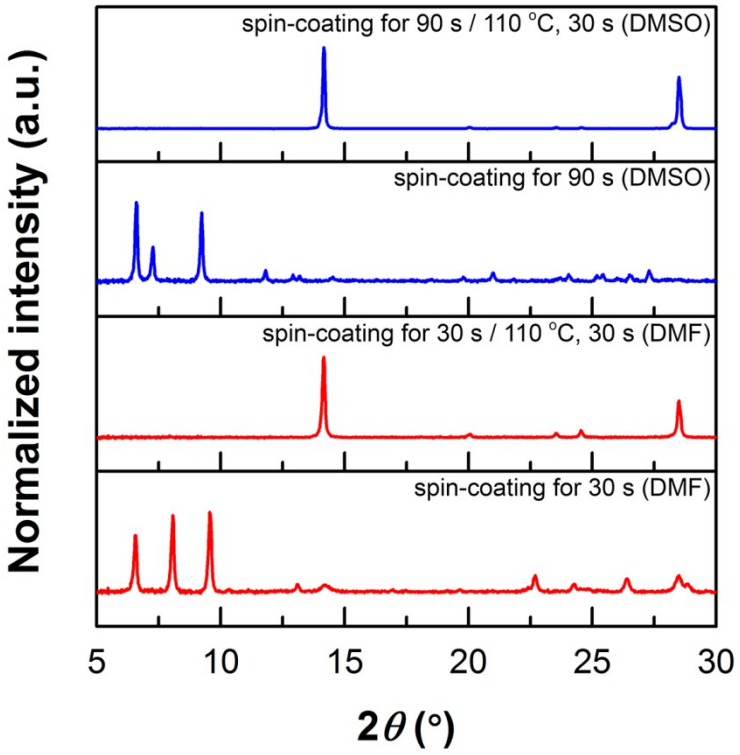

Fig. S3. XRD patterns of films fabricated from DMF and DMSO solution. The solidified films are prepared by spin-coating at 3000 rpm for 30 s (DMF) or 90 s (DMSO). When the solid films after spin-coating are thermally treated at 110 °C for 30 s, all peaks corresponding to CH_3NH_3I–PbI_2–solvent complex crystal completely disappear.

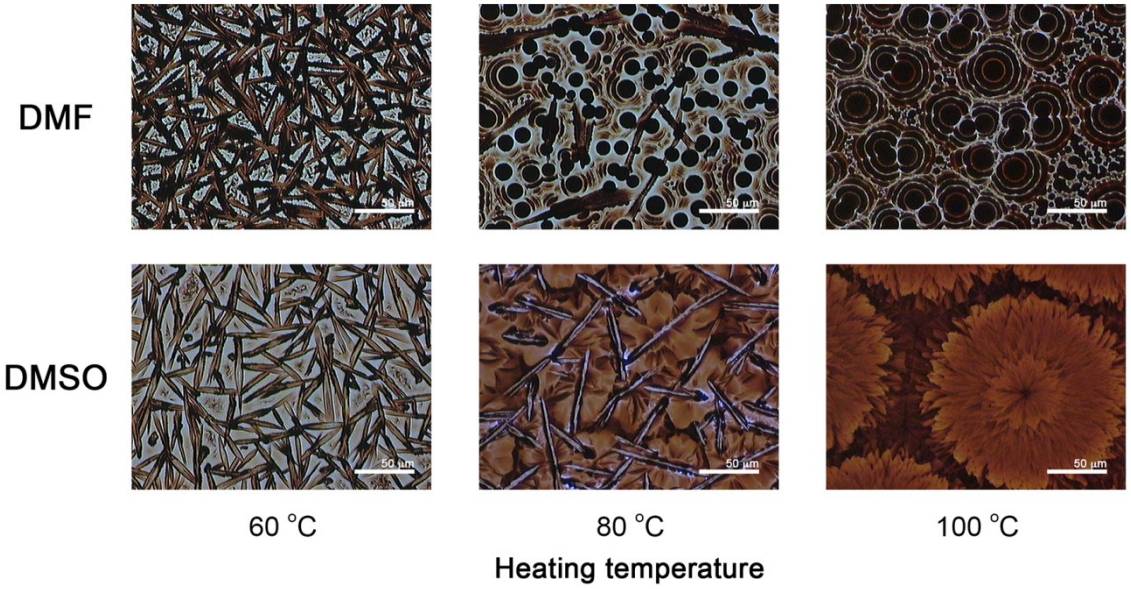

Fig. S4. OM images of $CH_3NH_3PbI_3$ films prepared from DMF and DMSO solution. The films are prepared by heating the liquid films, which are prepared by spin-coating at 3000 rpm for 3 s (DMF) or for 30 s (DMSO), at 60, 80 and 100 °C.

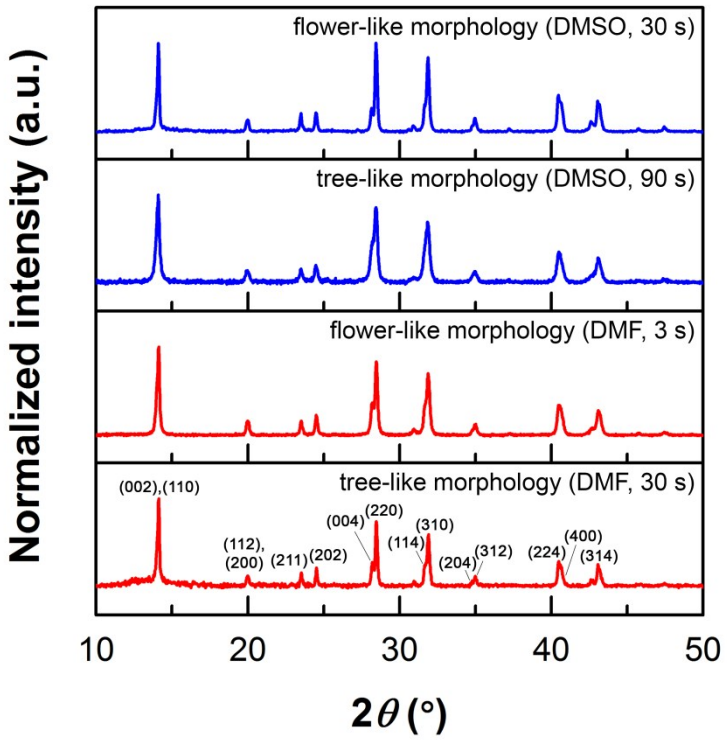

Fig. S5. Powder XRD patterns of $CH_3NH_3PbI_3$ films with flower-like and tree-like morphology fabricated from DMF and DMSO solution. All films are thermally treated at 110 °C for 30 s after spin-coating. Films with flower-like and tree-like morphologies are ground for powder samples.

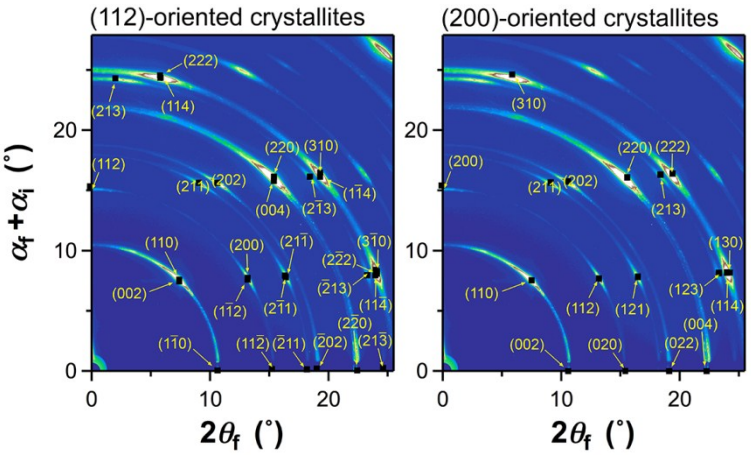

Fig. S6. Assignment of peaks showing preferred orientation of $CH_3NH_3PbI_3$ crystallites in films. The films with flower-like morphology are prepared from DMSO solution.

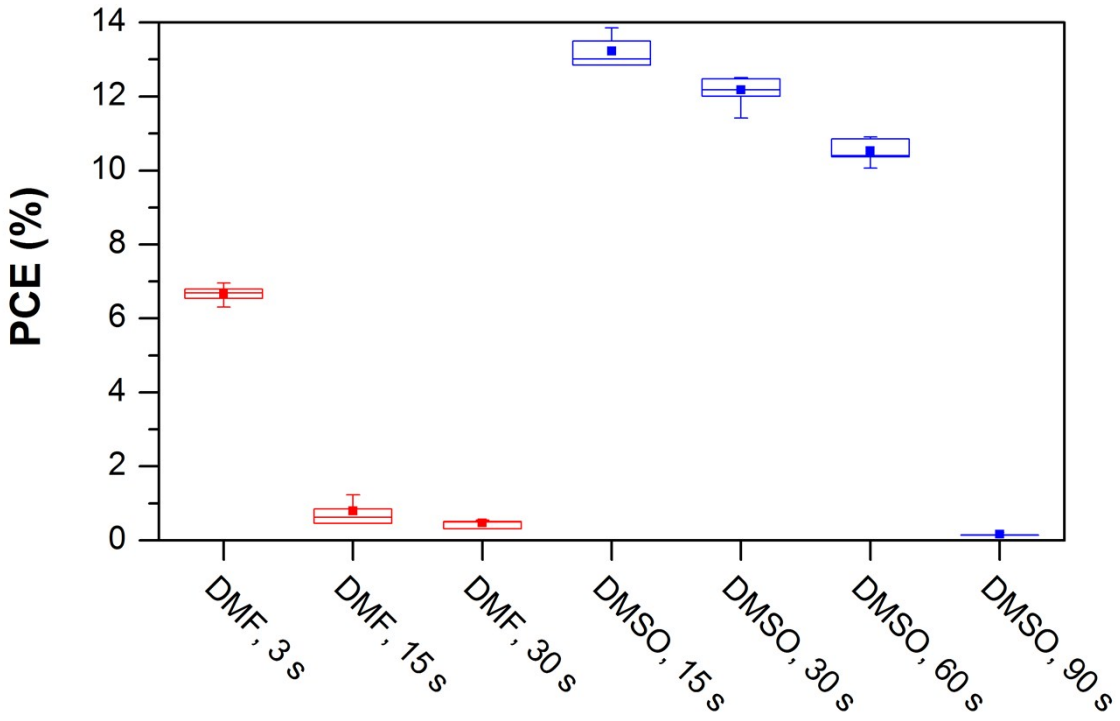

Fig. S7. Statistical analysis of the power conversion efficiencies of the $CH_3NH_3PbI_3$ perovskite solar cells depending on solvent and spin-coating time.

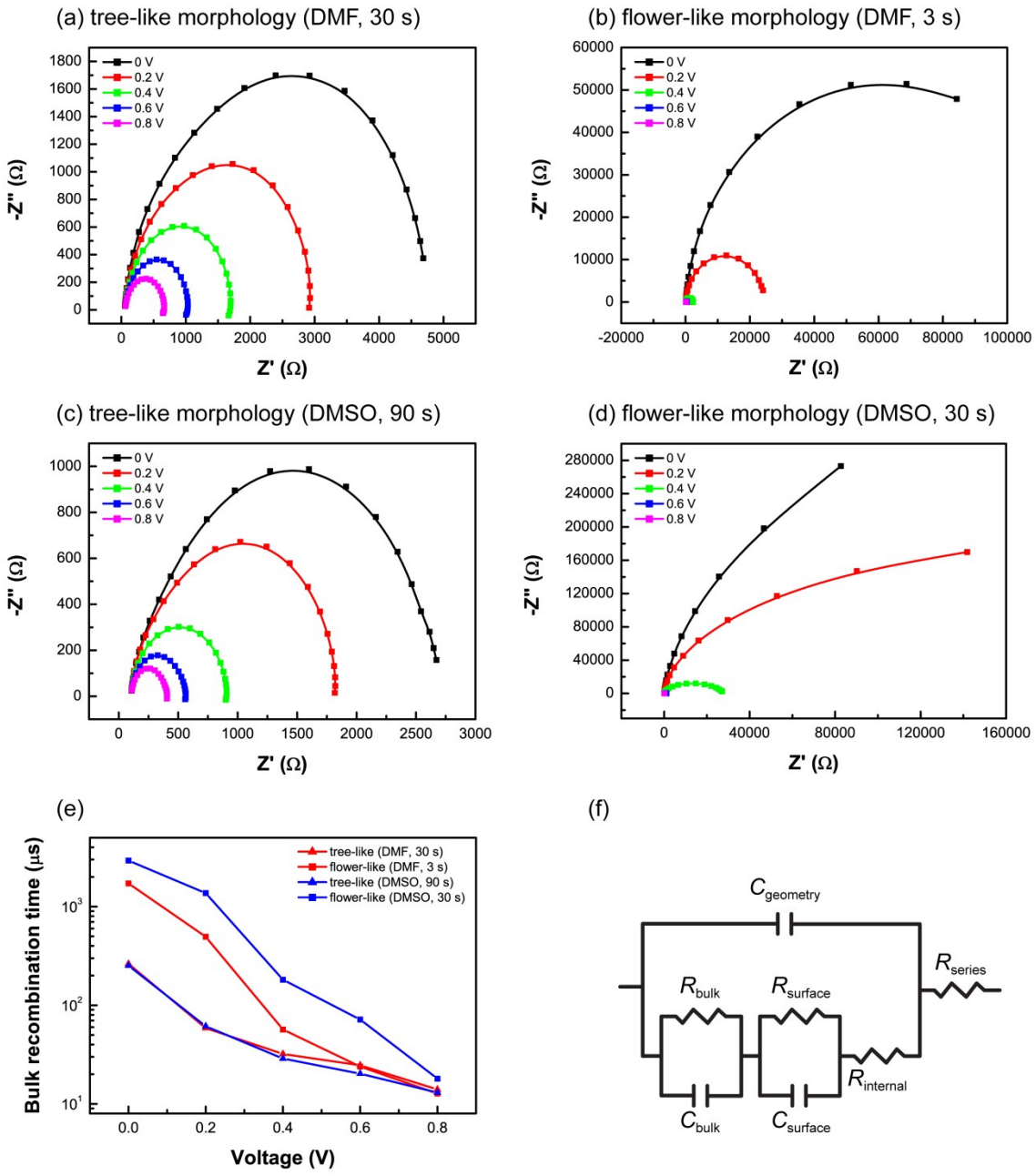

Fig. S8. Nyquist plots of $CH_3NH_3PbI_3$ solar cells with (a–d) different morphology and processing solvent under different applied voltage. (e) Bulk recombination times are calculated by fitting the Nyquist plot using the equivalent circuit (f).

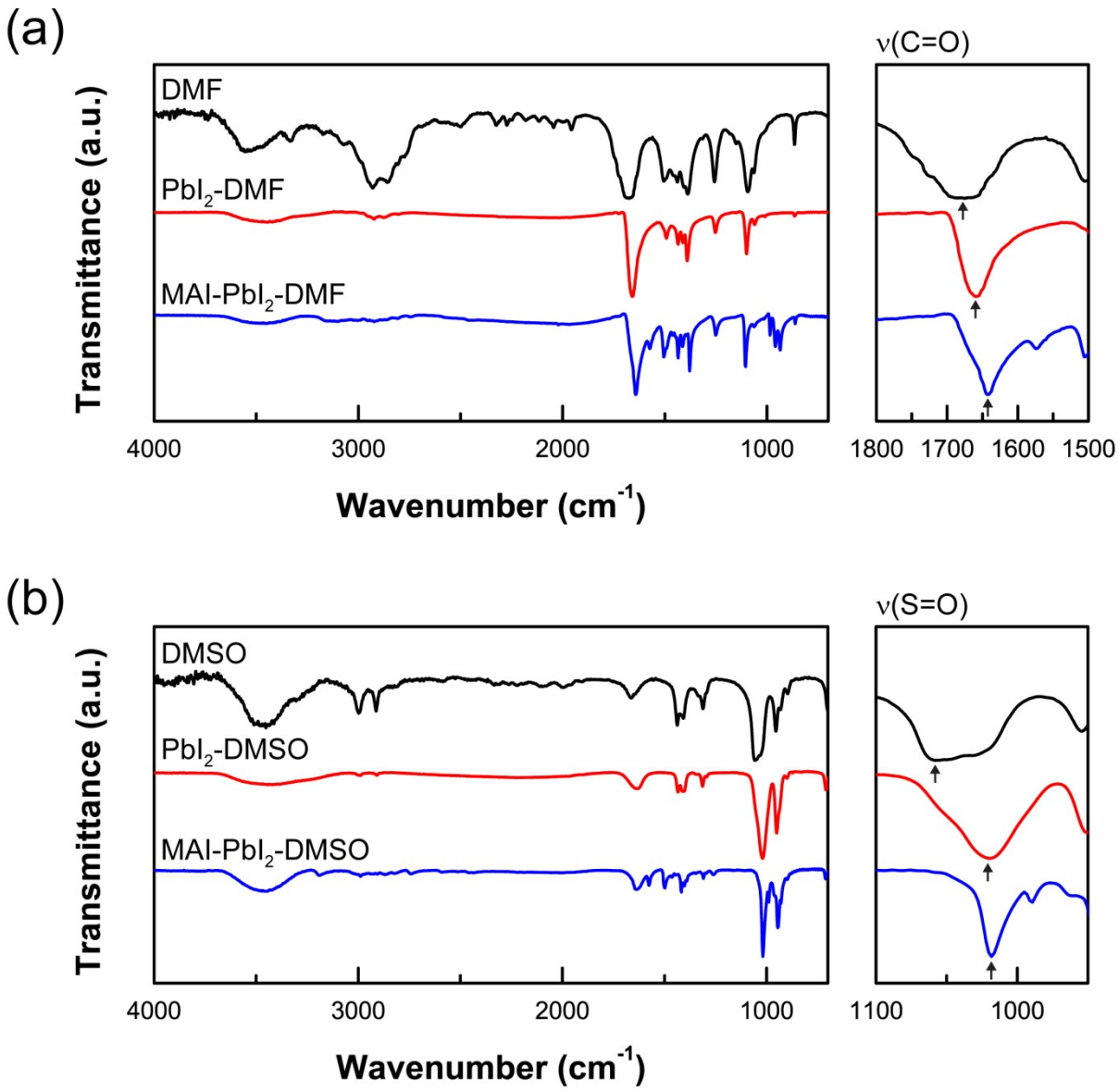

Fig. S9. FT-IR spectra of (a) DMF (solution), PbI_2–DMF (powder), CH_3NH_3I–PbI_2–DMF (powder) and (b) DMSO (solution), PbI_2–DMSO (powder), CH_3NH_3I–PbI_2–DMSO (powder).